

Figure 10.23 Isothermal transformation diagram for an alloy steel (type 4340): A, austenite; B, bainite; P, pearlite; M, martensite; F, proeutectoid ferrite.

[Adapted from H. Boyer (Editor), *Atlas of Isothermal Transformation and Cooling Transformation Diagrams*, 1977. Reproduced by permission of ASM International, Materials Park, OH.]

EXAMPLE PROBLEM 10.3

Microstructural Determinations for Three Isothermal Heat Treatments

Using the isothermal transformation diagram for an iron-carbon alloy of eutectoid composition (Figure 10.22), specify the nature of the final microstructure (in terms of microconstituents present and approximate percentages) of a small specimen that has been subjected to the following time-temperature treatments. In each case, assume that the specimen begins at 760°C (1400°F) and that it has been held at this temperature long enough to have achieved a complete and homogeneous austenitic structure.

- Rapidly cool to 350°C (660°F), hold for 10^4 s, and quench to room temperature.
- Rapidly cool to 250°C (480°F), hold for 100 s, and quench to room temperature.
- Rapidly cool to 650°C (1200°F), hold for 20 s, rapidly cool to 400°C (750°F), hold for 10^3 s, and quench to room temperature.

Solution

The time-temperature paths for all three treatments are shown in Figure 10.24. In each case, the initial cooling is rapid enough to prevent any transformation from occurring.

- At 350°C austenite isothermally transforms into bainite; this reaction begins after about 10 s and reaches completion at about 500 s elapsed time. Therefore, by 10^4 s, as stipulated in this problem, 100% of the specimen is bainite, and no further transformation is

WileyPLUS

Tutorial Video:
Isothermal
Transformation
Diagrams
Which Heat
Treatment Goes
with Which
Microstructure?

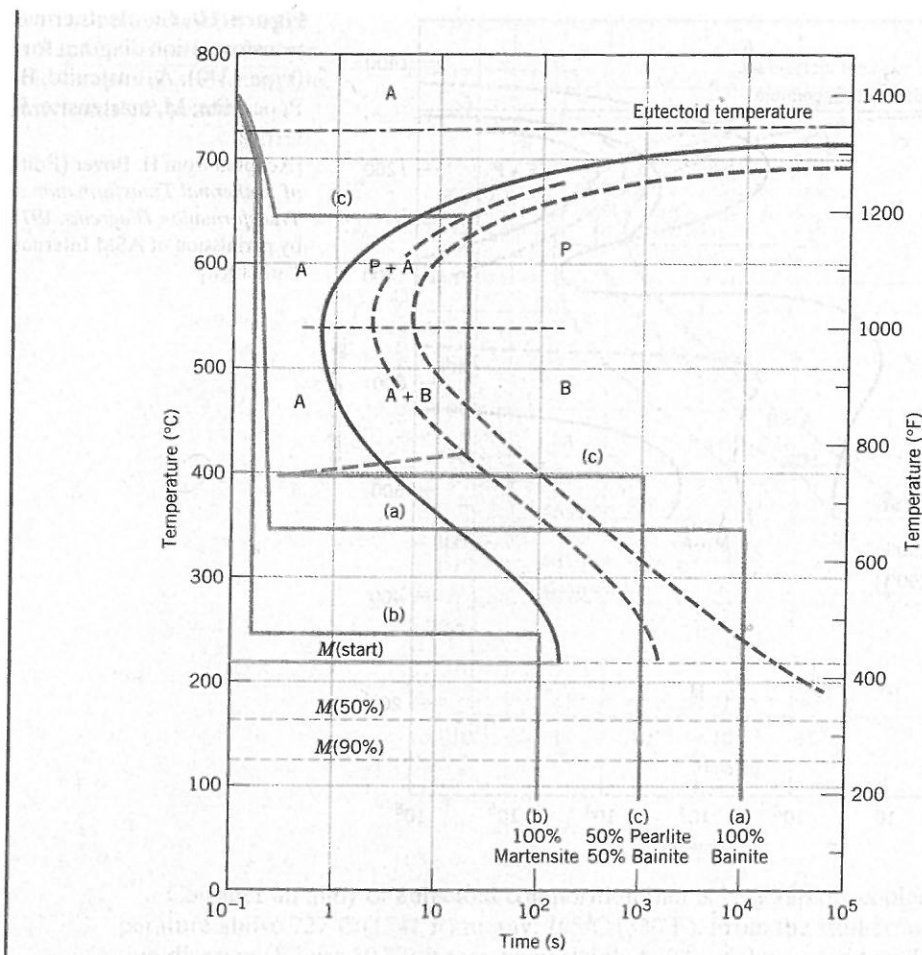


Figure 10.24 Isothermal transformation diagram for an iron–carbon alloy of eutectoid composition and the isothermal heat treatments (a), (b), and (c) in Example Problem 10.3.

possible, even though the final quenching line passes through the martensite region of the diagram.

- (b) In this case, it takes about 150 s at 250°C for the bainite transformation to begin, so that at 100 s the specimen is still 100% austenite. As the specimen is cooled through the martensite region, beginning at about 215°C, progressively more of the austenite instantaneously transforms into martensite. This transformation is complete by the time room temperature is reached, such that the final microstructure is 100% martensite.
- (c) For the isothermal line at 650°C, pearlite begins to form after about 7 s; by the time 20 s has elapsed, only approximately 50% of the specimen has transformed to pearlite. The rapid cool to 400°C is indicated by the vertical line; during this cooling, very little, if any, remaining austenite will transform to either pearlite or bainite, even though the cooling line passes through pearlite and bainite regions of the diagram. At 400°C, we begin timing at essentially zero time (as indicated in Figure 10.24); thus, by the time 10^3 s has elapsed, all of the remaining 50% austenite will have completely transformed to bainite. Upon quenching to room temperature, any further transformation is not possible inasmuch as no austenite remains, and so the final microstructure at room temperature consists of 50% pearlite and 50% bainite.

Concept Check 10.3 Make a copy of the isothermal transformation diagram for an iron-carbon alloy of eutectoid composition (Figure 10.22) and then sketch and label on this diagram a time-temperature path that will produce 100% fine pearlite.

[The answer may be found at www.wiley.com/college/callister (Student Companion Site).]

10.6 CONTINUOUS-COOLING TRANSFORMATION DIAGRAMS

continuous-cooling transformation diagram

Isothermal heat treatments are not the most practical to conduct because an alloy must be rapidly cooled to and maintained at an elevated temperature from a higher temperature above the eutectoid. Most heat treatments for steels involve the continuous cooling of a specimen to room temperature. An isothermal transformation diagram is valid only for conditions of constant temperature; this diagram must be modified for transformations that occur as the temperature is constantly changing. For continuous cooling, the time required for a reaction to begin and end is delayed. Thus the isothermal curves are shifted to longer times and lower temperatures, as indicated in Figure 10.25 for an iron-carbon alloy of eutectoid composition. A plot containing such modified beginning and ending reaction curves is termed a **continuous-cooling transformation (CCT)** diagram. Some control may be maintained over the rate of temperature change, depending on the cooling environment. Two cooling curves corresponding to moderately fast and

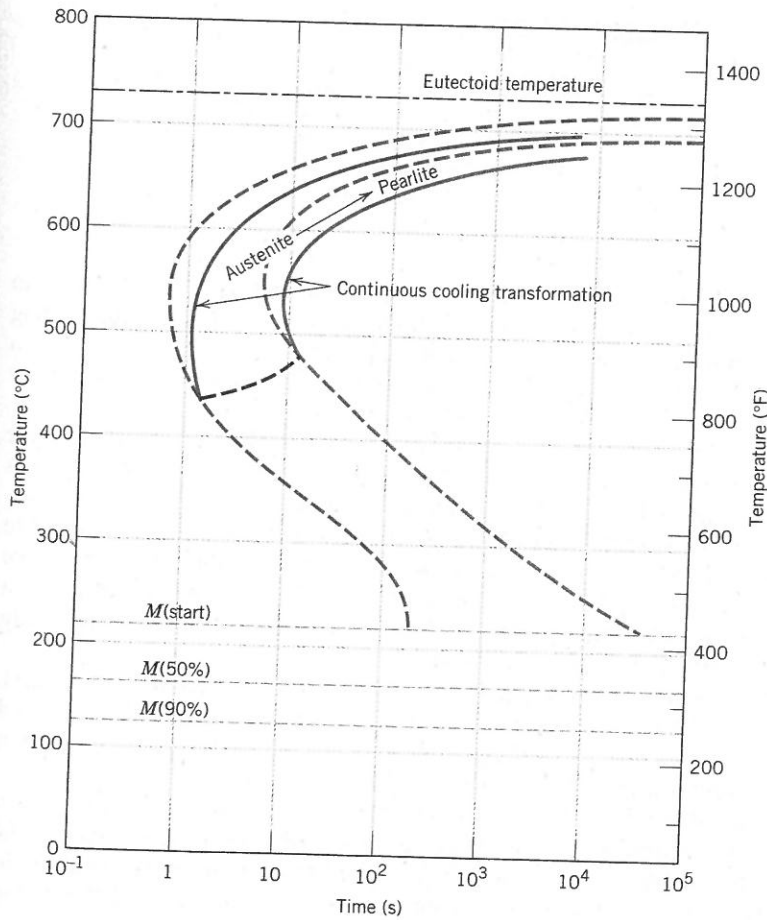
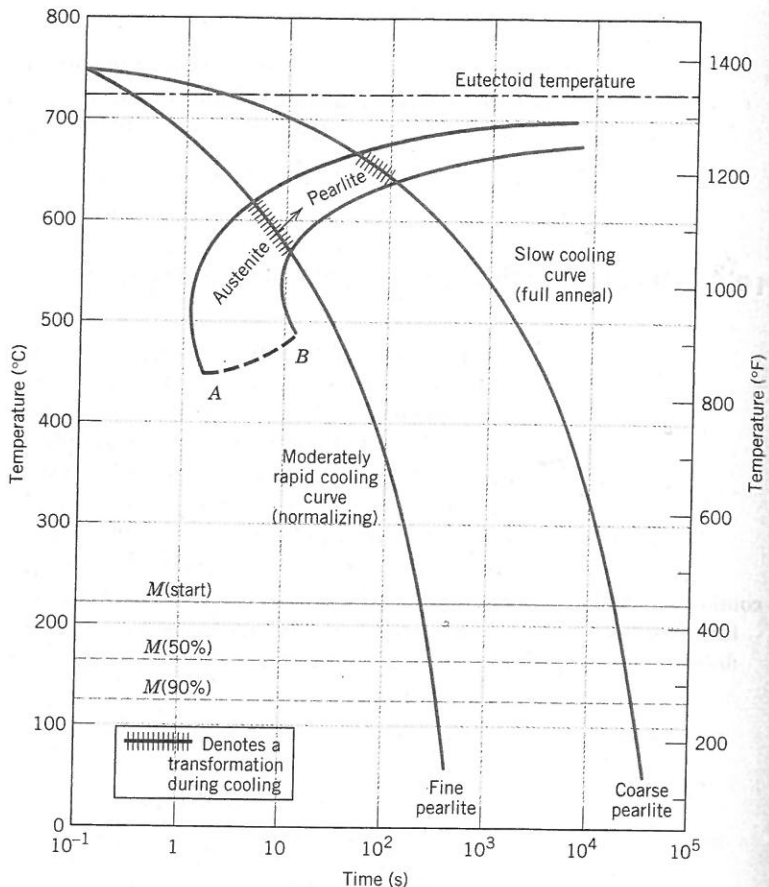


Figure 10.25 Superimposition of isothermal and continuous-cooling transformation diagrams for a eutectoid iron-carbon alloy.

[Adapted from H. Boyer (Editor), *Atlas of Isothermal Transformation and Cooling Transformation Diagrams*, 1977. Reproduced by permission of ASM International, Materials Park, OH.]

Figure 10.26 Moderately rapid and slow cooling curves superimposed on a continuous-cooling transformation diagram for a eutectoid iron-carbon alloy.



slow rates are superimposed and labeled in Figure 10.26, again for a eutectoid steel. The transformation starts after a time period corresponding to the intersection of the cooling curve with the beginning reaction curve and concludes upon crossing the completion transformation curve. The microstructural products for the moderately rapid and slow cooling rate curves in Figure 10.26 are fine and coarse pearlite, respectively.

Normally, bainite will not form when an alloy of eutectoid composition or, for that matter, any plain carbon steel is continuously cooled to room temperature. This is because all of the austenite has transformed into pearlite by the time the bainite transformation has become possible. Thus, the region representing the austenite-pearlite transformation terminates just below the nose (Figure 10.26), as indicated by the curve AB. For any cooling curve passing through AB in Figure 10.26, the transformation ceases at the point of intersection; with continued cooling, the unreacted austenite begins transforming into martensite upon crossing the M(start) line.

With regard to the representation of the martensitic transformation, the M(start), M(50%), and M(90%) lines occur at identical temperatures for both isothermal and continuous-cooling transformation diagrams. This may be verified for an iron-carbon alloy of eutectoid composition by comparison of Figures 10.22 and 10.25.

For the continuous cooling of a steel alloy, there exists a critical quenching rate, which represents the minimum rate of quenching that produces a totally martensitic structure. This critical cooling rate, when included on the continuous transformation diagram, just misses the nose at which the pearlite transformation begins, as illustrated in

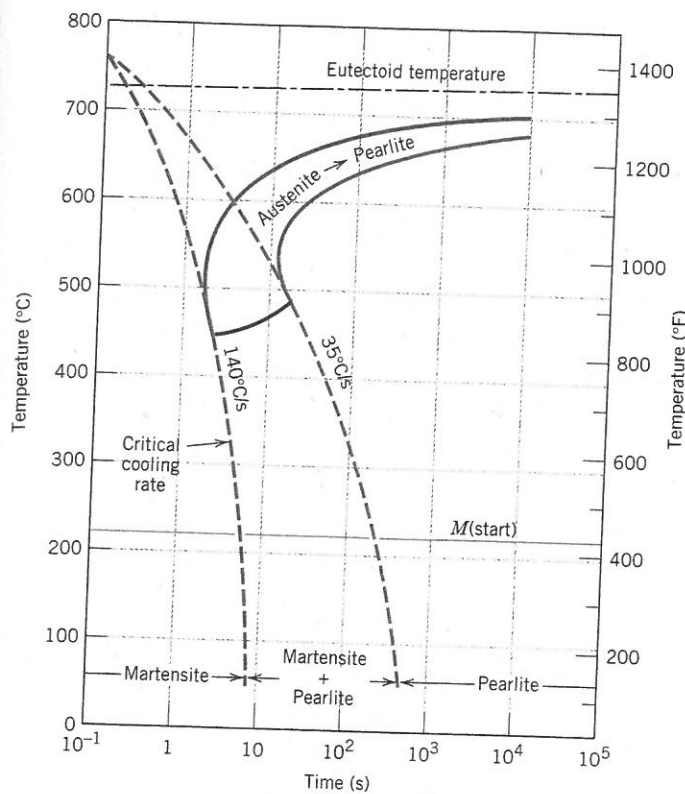


Figure 10.27 Continuous-cooling transformation diagram for a eutectoid iron–carbon alloy and superimposed cooling curves, demonstrating the dependence of the final microstructure on the transformations that occur during cooling.

Figure 10.27. As the figure also shows, only martensite exists for quenching rates greater than the critical one; in addition, there is a range of rates over which both pearlite and martensite are produced. Finally, a totally pearlitic structure develops for low cooling rates.

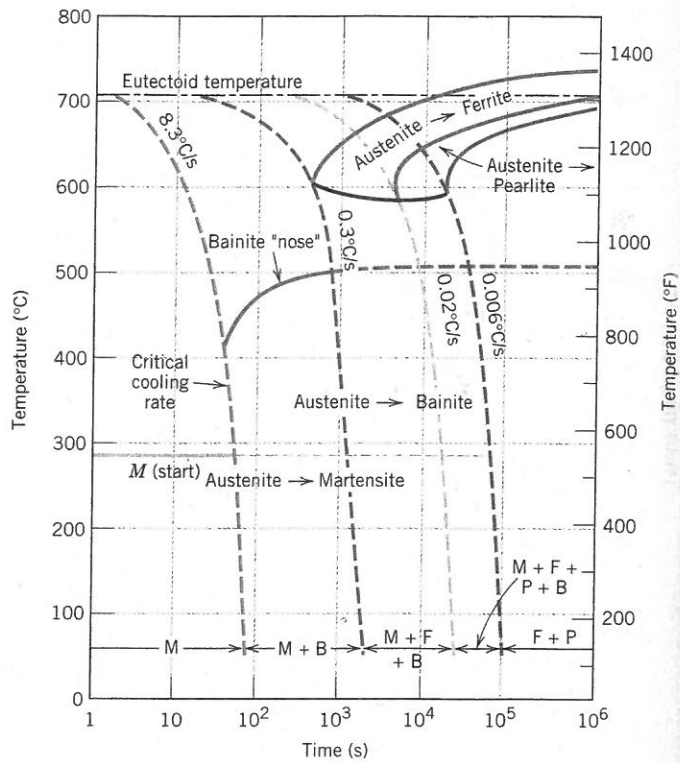
Carbon and other alloying elements also shift the pearlite (as well as the proeutectoid phase) and bainite noses to longer times, thus decreasing the critical cooling rate. In fact, one of the reasons for alloying steels is to facilitate the formation of martensite so that totally martensitic structures can develop in relatively thick cross sections. Figure 10.28 shows the continuous-cooling transformation diagram for the same alloy steel for which the isothermal transformation diagram is presented in Figure 10.23. The presence of the bainite nose accounts for the possibility of formation of bainite for a continuous-cooling heat treatment. Several cooling curves superimposed on Figure 10.28 indicate the critical cooling rate, and also how the transformation behavior and final microstructure are influenced by the rate of cooling.

Of interest, the critical cooling rate is decreased even by the presence of carbon. In fact, iron–carbon alloys containing less than about 0.25 wt% carbon are not normally heat-treated to form martensite because quenching rates too rapid to be practical are required. Other alloying elements that are particularly effective in rendering steels heat-treatable are chromium, nickel, molybdenum, manganese, silicon, and tungsten; however, these elements must be in solid solution with the austenite at the time of quenching.

In summary, isothermal and continuous-cooling transformation diagrams are, in a sense, phase diagrams in which the parameter of time is introduced. Each is experimentally determined for an alloy of specified composition, the variables being temperature and time. These diagrams allow prediction of the microstructure after some time period for constant-temperature and continuous-cooling heat treatments, respectively.

Figure 10.28 Continuous-cooling transformation diagram for an alloy steel (type 4340) and several superimposed cooling curves demonstrating dependence of the final microstructure of this alloy on the transformations that occur during cooling.

[Adapted from H. E. McGannon (Editor), *The Making, Shaping and Treating of Steel*, 9th edition, United States Steel Corporation, Pittsburgh, 1971, p. 1096.]



Concept Check 10.4 Briefly describe the simplest continuous cooling heat treatment procedure that would be used to convert a 4340 steel from (martensite + bainite) into (ferrite + pearlite).

[The answer may be found at www.wiley.com/college/callister (Student Companion Site).]

10.7 MECHANICAL BEHAVIOR OF IRON-CARBON ALLOYS

We now discuss the mechanical behavior of iron-carbon alloys having the microstructures discussed heretofore—namely, fine and coarse pearlite, spheroidite, bainite, and martensite. For all but martensite, two phases are present (ferrite and cementite), and so an opportunity is provided to explore several mechanical property-microstructure relationships that exist for these alloys.

Pearlite

Cementite is much harder but more brittle than ferrite. Thus, increasing the fraction of Fe_3C in a steel alloy while holding other microstructural elements constant will result in a harder and stronger material. This is demonstrated in Figure 10.29a, in which the tensile and yield strengths and the Brinell hardness number are plotted as a function of the weight percent carbon (or equivalently as the percentage of Fe_3C) for steels that are composed of fine pearlite. All three parameters increase with increasing carbon concentration. Inasmuch as cementite is more brittle, increasing its content results in a decrease in both ductility and toughness (or impact energy). These effects are shown in Figure 10.29b for the same fine pearlitic steels.

The layer thickness of each of the ferrite and cementite phases in the microstructure also influences the mechanical behavior of the material. Fine pearlite is harder and

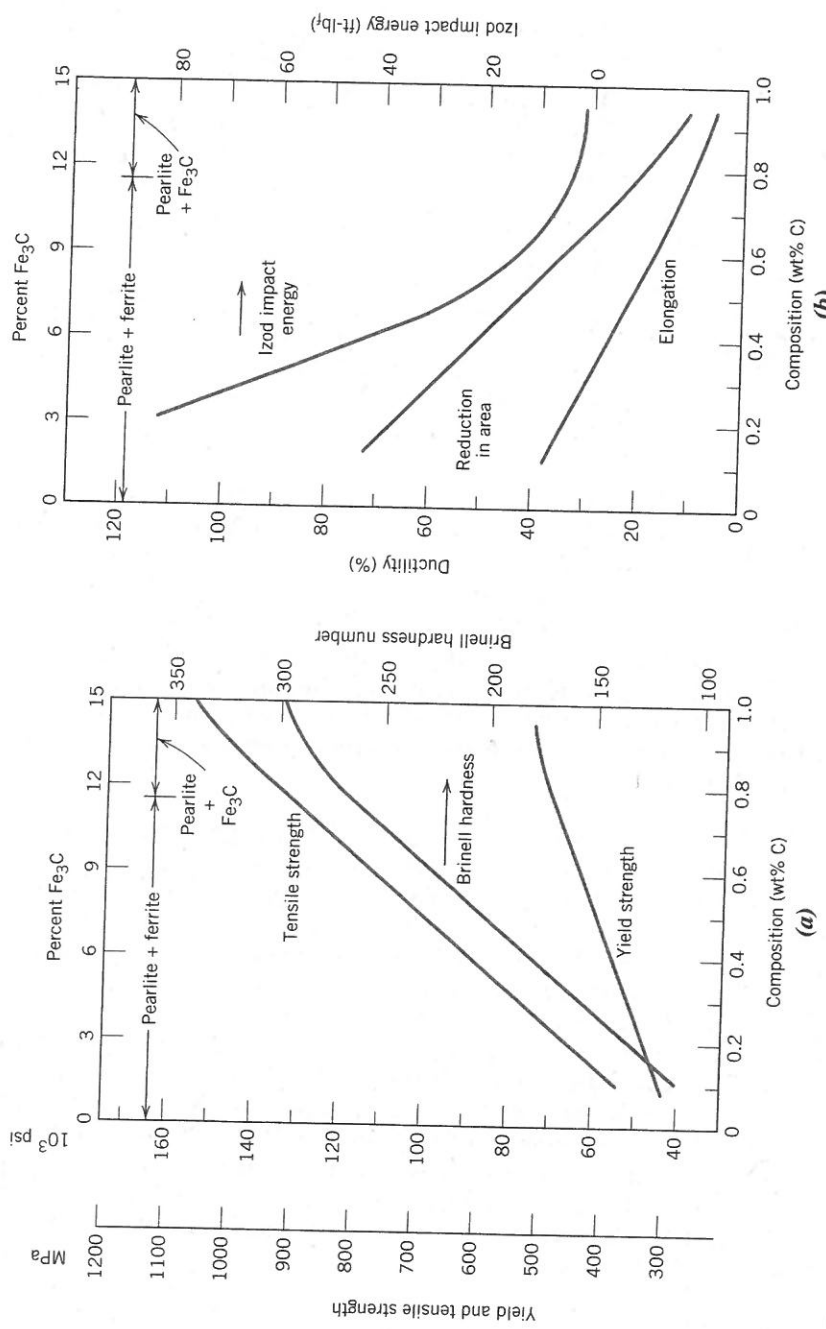


Figure 10.29 (a) Yield strength, tensile strength, and Brinell hardness versus carbon concentration for plain carbon steels having microstructures consisting of fine pearlite. (b) Ductility (%EL and %RA) and Izod impact energy versus carbon concentration for plain carbon steels having microstructures consisting of fine pearlite.
[Data taken from *Metals Handbook: Heat Treating*, Vol. 4, 9th edition, V. Masseria (Managing Editor), 1981. Reproduced by permission of ASM International, Materials Park, OH.]

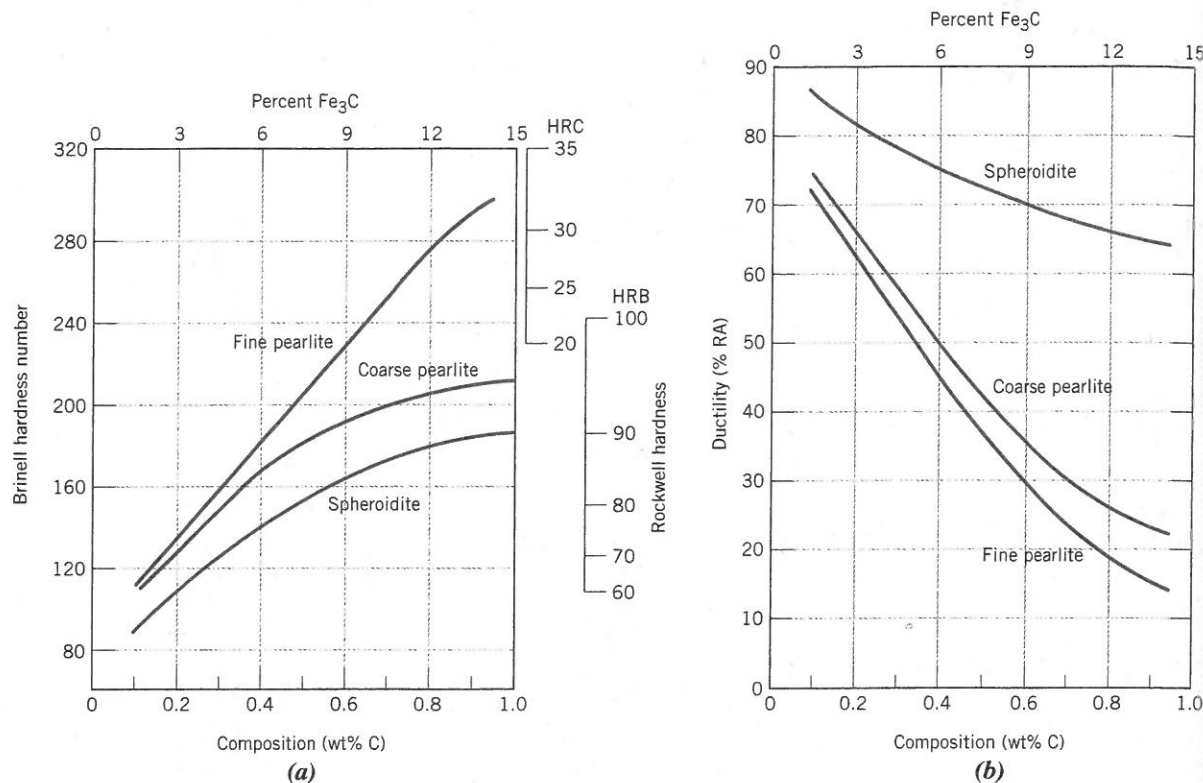


Figure 10.30 (a) Brinell and Rockwell hardness as a function of carbon concentration for plain carbon steels having fine and coarse pearlite as well as spheroidite microstructures. (b) Ductility (%RA) as a function of carbon concentration for plain carbon steels having fine and coarse pearlite as well as spheroidite microstructures. [Data taken from *Metals Handbook: Heat Treating*, Vol. 4, 9th edition, V. Masseria (Managing Editor), 1981. Reproduced by permission of ASM International, Materials Park, OH.]

stronger than coarse pearlite, as demonstrated by the upper two curves of Figure 10.30a, which plots hardness versus the carbon concentration.

The reasons for this behavior relate to phenomena that occur at the α -Fe₃C phase boundaries. First, there is a large degree of adherence between the two phases across a boundary. Therefore, the strong and rigid cementite phase severely restricts deformation of the softer ferrite phase in the regions adjacent to the boundary; thus the cementite may be said to reinforce the ferrite. The degree of this reinforcement is substantially higher in fine pearlite because of the greater phase boundary area per unit volume of material. In addition, phase boundaries serve as barriers to dislocation motion in much the same way as grain boundaries (Section 7.8). For fine pearlite there are more boundaries through which a dislocation must pass during plastic deformation. Thus, the greater reinforcement and restriction of dislocation motion in fine pearlite account for its greater hardness and strength.

Coarse pearlite is more ductile than fine pearlite, as illustrated in Figure 10.30b, which plots percentage reduction in area versus carbon concentration for both microstructure types. This behavior results from the greater restriction to plastic deformation of the fine pearlite.

Spheroidite

Other elements of the microstructure relate to the shape and distribution of the phases. In this respect, the cementite phase has distinctly different shapes and arrangements in the pearlite and spheroidite microstructures (Figures 10.15 and 10.19). Alloys containing pearlitic microstructures have greater strength and hardness than do those with spheroidite. This is demonstrated in Figure 10.30a, which compares the hardness as a function of the

weight percent carbon for spheroidite with both the pearlite structure types. This behavior is again explained in terms of reinforcement at, and impedance to, dislocation motion across the ferrite–cementite boundaries as discussed previously. There is less boundary area per unit volume in spheroidite, and consequently plastic deformation is not nearly as constrained, which gives rise to a relatively soft and weak material. In fact, of all steel alloys, those that are softest and weakest have a spheroidite microstructure.

As might be expected, spheroidized steels are extremely ductile, much more than either fine or coarse pearlite (Figure 10.30b). In addition, they are notably tough because any crack can encounter only a very small fraction of the brittle cementite particles as it propagates through the ductile ferrite matrix.

Bainite

Because bainitic steels have a finer structure (i.e., smaller α -ferrite and Fe_3C particles), they are generally stronger and harder than pearlitic steels; yet they exhibit a desirable combination of strength and ductility. Figures 10.31a and 10.31b show, respectively, the influence of transformation temperature on the strength/hardness and ductility for an iron–carbon alloy of eutectoid composition. Temperature ranges over which pearlite and bainite form (consistent with the isothermal transformation diagram for this alloy, Figure 10.18) are noted at the tops of Figures 10.31a and 10.31b.

Martensite

Of the various microstructures that may be produced for a given steel alloy, martensite is the hardest and strongest and, in addition, the most brittle; it has, in fact, negligible ductility. Its hardness is dependent on the carbon content, up to about 0.6 wt% as demonstrated in Figure 10.32, which plots the hardness of martensite and fine pearlite as a function of weight percent carbon. In contrast to pearlitic steels, the strength and hardness of martensite are not thought to be related to microstructure. Rather, these properties are attributed to the effectiveness of the interstitial carbon atoms in hindering dislocation motion (as a solid-solution effect, Section 7.9), and to the relatively few slip systems (along which dislocations move) for the BCT structure.

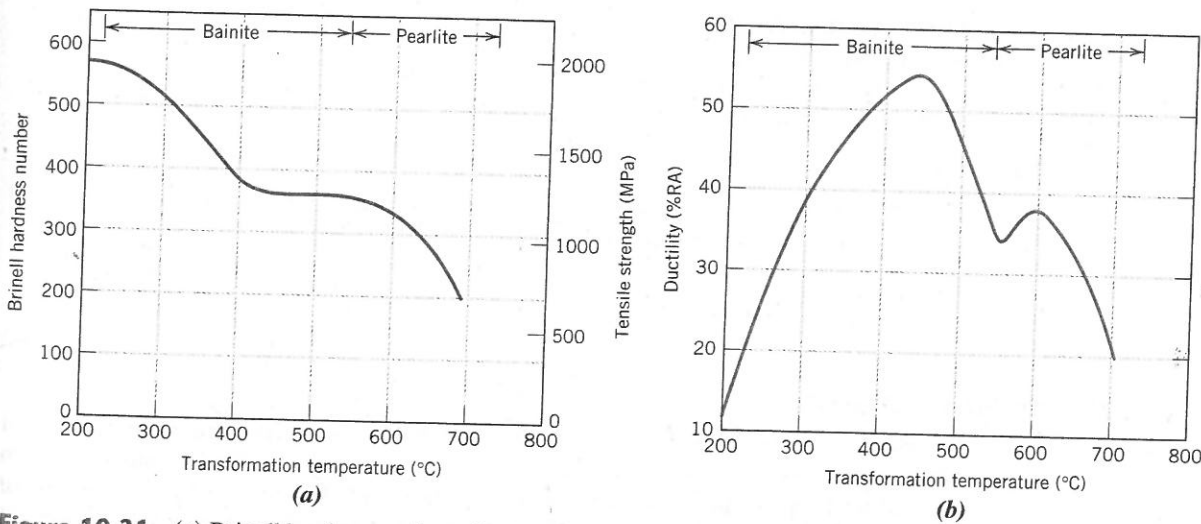
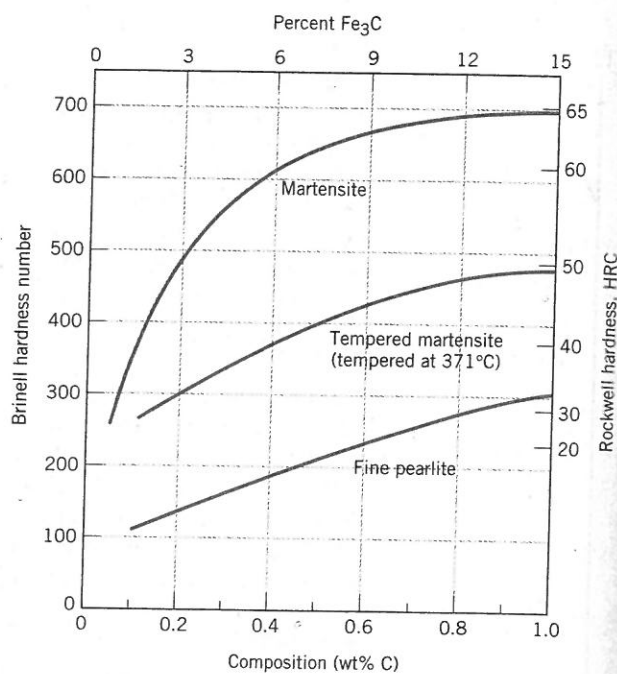


Figure 10.31 (a) Brinell hardness and tensile strength and (b) ductility (%RA) (at room temperature) as a function of isothermal transformation temperature for an iron–carbon alloy of eutectoid composition, taken over the temperature range at which bainitic and pearlitic microstructures form.
[Figure (a) Adapted from E. S. Davenport, "Isothermal Transformation in Steels," *Trans. ASM*, **27**, 1939, p. 847. Reprinted by permission of ASM International, Materials Park, OH.]

Figure 10.32 Hardness (at room temperature) as a function of carbon concentration for plain carbon martensitic, tempered martensitic [tempered at 371°C (700°F)], and pearlitic steels. (Adapted from Edgar C. Bain, *Functions of the Alloying Elements in Steel*, 1939; and R. A. Grange, C. R. Hribal, and L. F. Porter, *Metall. Trans. A*, Vol. 8A. Reproduced by permission of ASM International, Materials Park, OH.)



Austenite is slightly denser than martensite, and therefore, during the phase transformation upon quenching, there is a net volume increase. Consequently, relatively large pieces that are rapidly quenched may crack as a result of internal stresses; this becomes a problem especially when the carbon content is greater than about 0.5 wt%.

Concept Check 10.5 Rank the following iron–carbon alloys and associated microstructures from the highest to the lowest tensile strength:

- 0.25 wt% C with spheroidite
- 0.25 wt% C with coarse pearlite
- 0.6 wt% C with fine pearlite
- 0.6 wt% C with coarse pearlite

Justify this ranking.

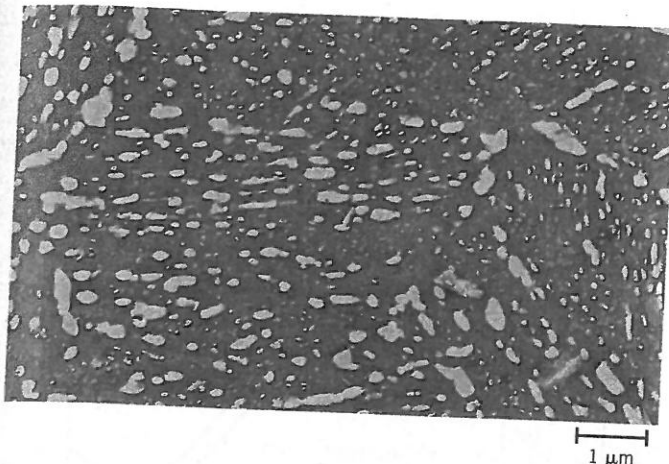
Concept Check 10.6 For a eutectoid steel, describe an isothermal heat treatment that would be required to produce a specimen having a hardness of 93 HRB.

[The answers may be found at www.wiley.com/college/callister (Student Companion Site).]

10.8 TEMPERED MARTENSITE

In the as-quenched state, martensite, in addition to being very hard, is so brittle that it cannot be used for most applications; also, any internal stresses that may have been introduced during quenching have a weakening effect. The ductility and toughness of martensite may be enhanced and these internal stresses relieved by a heat treatment known as *tempering*.

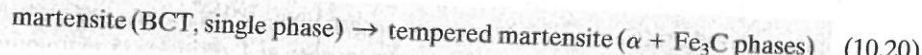
Tempering is accomplished by heating a martensitic steel to a temperature below the eutectoid for a specified time period. Normally, tempering is carried out at temperatures



tempered martensite

Martensite to tempered martensite transformation reaction

between 250°C and 650°C (480°F and 1200°F); internal stresses, however, may be relieved at temperatures as low as 200°C (390°F). This tempering heat treatment allows, by diffusional processes, the formation of **tempered martensite**, according to the reaction



where the single-phase BCT martensite, which is supersaturated with carbon, transforms into the tempered martensite, composed of the stable ferrite and cementite phases, as indicated on the iron-iron carbide phase diagram.

The microstructure of tempered martensite consists of extremely small and uniformly dispersed cementite particles embedded within a continuous ferrite matrix. This is similar to the microstructure of spheroidite except that the cementite particles are much, much smaller. An electron micrograph showing the microstructure of tempered martensite at a very high magnification is presented in Figure 10.33.

Tempered martensite may be nearly as hard and strong as martensite but with substantially enhanced ductility and toughness. For example, the hardness-versus-weight percent carbon plot of Figure 10.32 includes a curve for tempered martensite. The hardness and strength may be explained by the large ferrite-cementite phase boundary area per unit volume that exists for the very fine and numerous cementite particles. Again, the hard cementite phase reinforces the ferrite matrix along the boundaries, and these boundaries also act as barriers to dislocation motion during plastic deformation. The continuous ferrite phase is also very ductile and relatively tough, which accounts for the improvement of these two properties for tempered martensite.

The size of the cementite particles influences the mechanical behavior of tempered martensite; increasing the particle size decreases the ferrite-cementite phase boundary area and, consequently, results in a softer and weaker material yet one that is tougher and more ductile. Furthermore, the tempering heat treatment determines the size of the cementite particles. Heat treatment variables are temperature and time, and most treatments are constant-temperature processes. Because carbon diffusion is involved in the martensite-tempered martensite transformation, increasing the temperature accelerates diffusion, the rate of cementite particle growth, and, subsequently, the rate of softening. The dependence of tensile and yield strength and ductility on tempering temperature for an alloy steel is shown in Figure 10.34. Before tempering, the material was quenched in oil to produce the martensitic structure; the tempering time at each temperature was 1 h. This type of tempering data is ordinarily provided by the steel manufacturer.

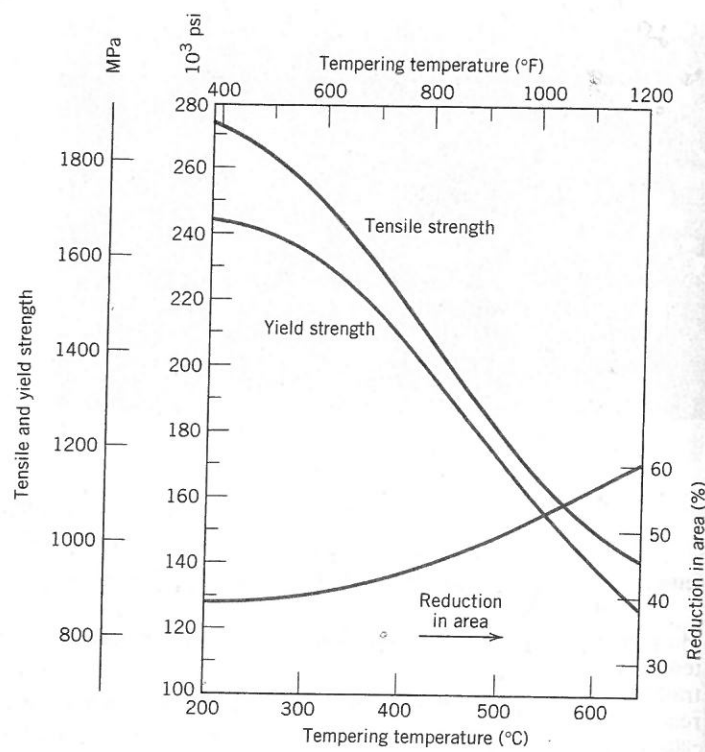
The time dependence of hardness at several different temperatures is presented in Figure 10.35 for a water-quenched steel of eutectoid composition; the time scale is

Figure 10.33 Electron micrograph of tempered martensite. Tempering was carried out at 594°C (1100°F). The small particles are the cementite phase; the matrix phase is α -ferrite. 9300 \times .

(Copyright 1971 by United States Steel Corporation.)

Figure 10.34 Tensile and yield strengths and ductility (%RA) (at room temperature) versus tempering temperature for an oil-quenched alloy steel (type 4340).

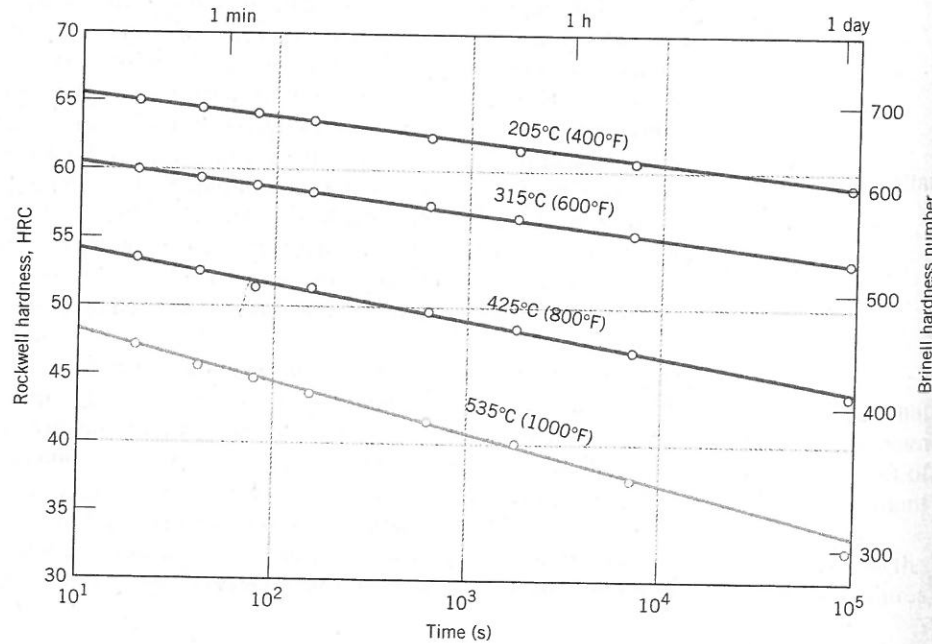
(Adapted from Edgar C. Bain, *Functions of the Alloying Elements in Steel*, 1939. Reproduced by permission of ASM International, Materials Park, OH.)



logarithmic. With increasing time the hardness decreases, which corresponds to the growth and coalescence of the cementite particles. At temperatures approaching the eutectoid [700°C (1300°F)] and after several hours, the microstructure will become spheroiditic (Figure 10.19), with large cementite spheroids embedded within the continuous ferrite phase. Correspondingly, overtempered martensite is relatively soft and ductile.

Figure 10.35 Hardness (at room temperature) versus tempering time for a water-quenched eutectoid plain carbon (1080) steel.

(Adapted from Edgar C. Bain, *Functions of the Alloying Elements in Steel*, American Society for Metals, 1939, p. 233.)



Concept Check 10.7 A steel alloy is quenched from a temperature within the austenite phase region into water at room temperature so as to form martensite; the alloy is subsequently tempered at an elevated temperature, which is held constant.

- Make a schematic plot showing how room-temperature ductility varies with the logarithm of tempering time at the elevated temperature. (Be sure to label your axes.)
- Superimpose and label on this same plot the room-temperature behavior resulting from tempering at a higher temperature and briefly explain the difference in behavior at these two temperatures.

[The answer may be found at www.wiley.com/college/callister (Student Companion Site).]

The tempering of some steels may result in a reduction of toughness as measured by impact tests (Section 8.6); this is termed *temper embrittlement*. The phenomenon occurs when the steel is tempered at a temperature above about 575°C (1070°F) followed by slow cooling to room temperature, or when tempering is carried out at between approximately 375°C and 575°C (700°F and 1070°F). Steel alloys that are susceptible to temper embrittlement have been found to contain appreciable concentrations of the alloying elements manganese, nickel, or chromium and, in addition, one or more of antimony, phosphorus, arsenic, and tin as impurities in relatively low concentrations. The presence of these alloying elements and impurities shifts the ductile-to-brittle transition to significantly higher temperatures; the ambient temperature thus lies below this transition in the brittle regime. It has been observed that crack propagation of these embrittled materials is *intergranular* (Figure 8.7)—that is, the fracture path is along the grain boundaries of the precursor austenite phase. Furthermore, alloy and impurity elements have been found to preferentially segregate in these regions.

Temper embrittlement may be avoided by (1) compositional control and/or (2) tempering above 575°C or below 375°C, followed by quenching to room temperature. Furthermore, the toughness of steels that have been embrittled may be improved significantly by heating to about 600°C (1100°F) and then rapidly cooling to below 300°C (570°F).

10.9 REVIEW OF PHASE TRANSFORMATIONS AND MECHANICAL PROPERTIES FOR IRON-CARBON ALLOYS

In this chapter, we discussed several different microstructures that may be produced in iron-carbon alloys depending on heat treatment. Figure 10.36 summarizes the

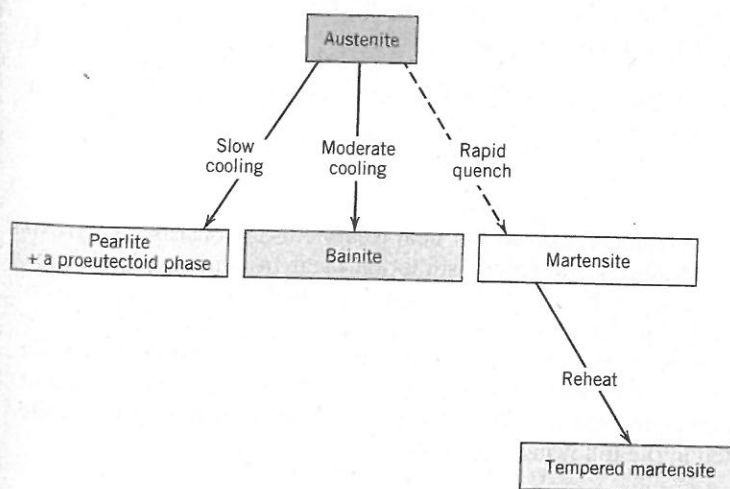


Figure 10.36 Possible transformations involving the decomposition of austenite. Solid arrows, transformations involving diffusion; dashed arrow, diffusionless transformation.

Table 10.2 Microstructures and Mechanical Properties for Iron–Carbon Alloys

<i>Microconstituent</i>	<i>Phases Present</i>	<i>Arrangement of Phases</i>	<i>Mechanical Properties (Relative)</i>
Spheroidite	α -Ferrite + Fe ₃ C	Relatively small Fe ₃ C spherelike particles in an α -ferrite matrix	Soft and ductile
Coarse pearlite	α -Ferrite + Fe ₃ C	Alternating layers of α -ferrite and Fe ₃ C that are relatively thick	Harder and stronger than spheroidite, but not as ductile as spheroidite
Fine pearlite	α -Ferrite + Fe ₃ C	Alternating layers of α -ferrite and Fe ₃ C that are relatively thin	Harder and stronger than coarse pearlite, but not as ductile as coarse pearlite
Bainite	α -Ferrite + Fe ₃ C	Very fine and elongated particles of Fe ₃ C in an α -ferrite matrix	Harder and stronger than fine pearlite; less hard than martensite; more ductile than martensite
Tempered martensite	α -Ferrite + Fe ₃ C	Very small Fe ₃ C spherelike particles in an α -ferrite matrix	Strong; not as hard as martensite, but much more ductile than martensite
Martensite	Body-centered, tetragonal, single phase	Needle-shaped grains	Very hard and very brittle

WileyPLUS

Tutorial Video:
Iron–Carbon Alloy
Microstructures
What are the
Differences
between the Various
Iron–Carbon Alloy
Microstructures?

transformation paths that produce these various microstructures. Here, it is assumed that pearlite, bainite, and martensite result from continuous-cooling treatments; furthermore, the formation of bainite is possible only for alloy steels (not plain carbon ones), as outlined earlier.

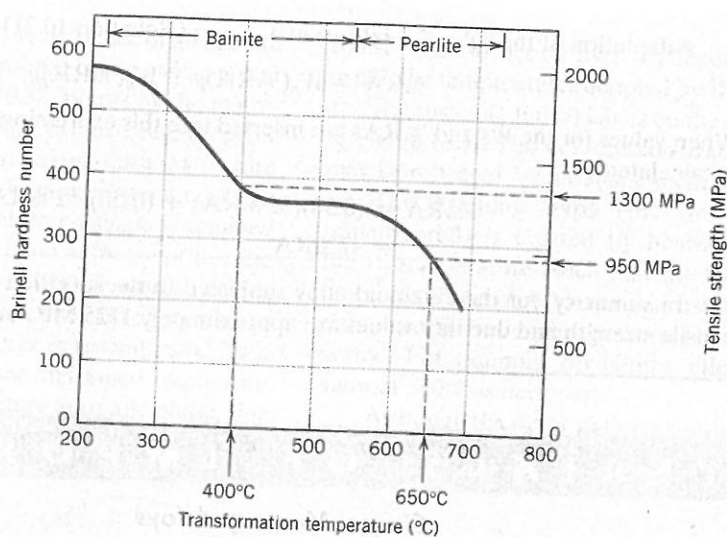
Microstructural characteristics and mechanical properties of the several microconstituents for iron–carbon alloys are summarized in Table 10.2.

EXAMPLE PROBLEM 10.4**Determination of Properties for a Eutectoid Fe–Fe₃C Alloy Subjected to an Isothermal Heat Treatment**

Determine the tensile strength and ductility (%RA) of a eutectoid Fe–Fe₃C alloy that has been subjected to heat treatment (c) in Example Problem 10.3.

Solution

According to Figure 10.24, the final microstructure for heat treatment (c) consists of approximately 50% pearlite that formed during the 650°C isothermal heat treatment, whereas the remaining 50% austenite transformed to bainite at 400°C; thus, the final microstructure is 50% pearlite and 50% bainite. The tensile strength may be determined using Figure 10.31a. For pearlite, which was formed at an isothermal transformation temperature of 650°C, the tensile strength is approximately 950 MPa, whereas using this same plot, the bainite that formed at 400°C has an approximate tensile strength of 1300 MPa. Determination of these two tensile strength values is demonstrated in the following illustration.



The tensile strength of this two-microconstituent alloy may be approximated using a "rule-of-mixtures" relationship—that is, the alloy tensile strength is equal to the fraction-weighted average of the two microconstituents, which may be expressed by the following equation:

$$\bar{TS} = W_p(TS)_p + W_b(TS)_b \quad (10.21)$$

Here,

\bar{TS} = tensile strength of the alloy,

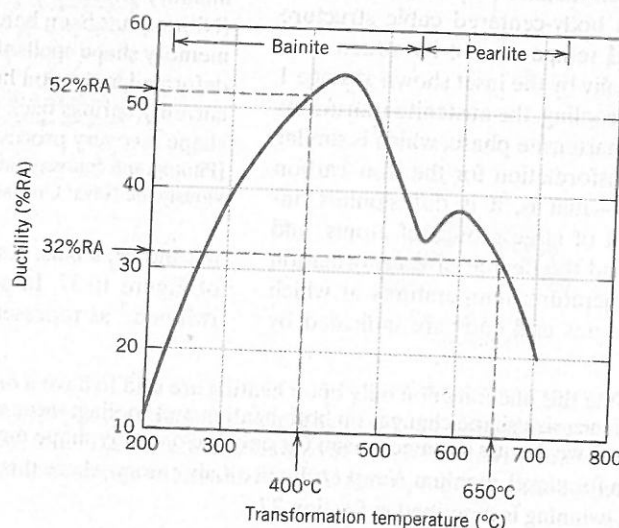
W_p and W_b = mass fractions of pearlite and bainite, respectively, and

$(TS)_p$ and $(TS)_b$ = tensile strengths of the respective microconstituents.

Thus, incorporating values for these four parameters into Equation 10.21 leads to the following alloy tensile strength:

$$\begin{aligned}\bar{TS} &= (0.50)(950 \text{ MPa}) + (0.50)(1300 \text{ MPa}) \\ &= 1125 \text{ MPa}\end{aligned}$$

This same technique is used for the computation of ductility. In this case, approximate ductility values for the two microconstituents, taken at 650°C (for pearlite) and 400°C (for bainite), are, respectively, 32%RA and 52%RA, as taken from the following adaptation of Figure 10.31b:



Adaptation of the rule-of-mixtures expression (Equation 10.21) for this case is as follows:

$$\% \overline{RA} = W_p(\% RA)_p + W_b(\% RA)_b$$

When values for the W s and $\% RAs$ are inserted into this expression, the approximate ductility is calculated as

$$\begin{aligned}\% \overline{RA} &= (0.50)(32\% RA) + (0.50)(52\% RA) \\ &= 42\% RA\end{aligned}$$

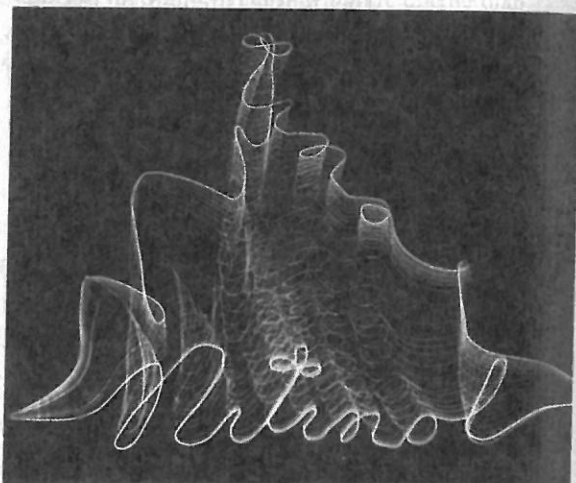
In summary, for the eutectoid alloy subjected to the specified isothermal heat treatment, tensile strength and ductility values are approximately 1125 MPa and 42% RA, respectively.

MATERIALS OF IMPORTANCE

Shape-Memory Alloys

A relatively new group of metals that exhibit an interesting (and practical) phenomenon are the *shape-memory alloys* (or SMAs). One of these materials, after being deformed, has the ability to return to its predeformed size and shape upon being subjected to an appropriate heat treatment—that is, the material “remembers” its previous size/shape. Deformation normally is carried out at a relatively low temperature, whereas shape memory occurs upon heating.⁵ Materials that have been found to be capable of recovering significant amounts of deformation (i.e., strain) are nickel–titanium alloys (Nitinol,⁶ is their trade name) and some copper-base alloys (Cu–Zn–Al and Cu–Al–Ni alloys).

A shape-memory alloy is polymorphic (Section 3.6)—that is, it may have two crystal structures (or phases), and the shape-memory effect involves phase transformations between them. One phase (termed an *austenite phase*) has a body-centered cubic structure that exists at elevated temperatures; its structure is represented schematically by the inset shown at stage 1 of Figure 10.37. Upon cooling, the austenite transforms spontaneously into a martensite phase, which is similar to the martensitic transformation for the iron–carbon system (Section 10.5)—that is, it is diffusionless, involves an orderly shift of large groups of atoms, and occurs very rapidly, and the degree of transformation is dependent on temperature; temperatures at which the transformation begins and ends are indicated by



Time-lapse photograph that demonstrates the shape-memory effect. A wire of a shape-memory alloy (Nitinol) has been bent and treated such that its memory shape spells the word *Nitinol*. The wire is then deformed and, upon heating (by passage of an electric current), springs back to its predeformed shape; this shape recovery process is recorded on the photograph. [Photograph courtesy the Naval Surface Warfare Center (previously the Naval Ordnance Laboratory)].

M_s and M_f labels, respectively, on the left vertical axis of Figure 10.37. In addition, this martensite is heavily twinned,⁷ as represented schematically by the stage 2

⁵Alloys that demonstrate this phenomenon only upon heating are said to have a *one-way* shape memory. Some of these materials experience size/shape changes on both heating and cooling; these are termed *two-way* shape memory alloys. In this discussion, we discuss the mechanism for only the one-way shape memory alloys.

⁶Nitinol is an acronym for nickel-titanium Naval Ordnance Laboratory, where this alloy was discovered.

⁷The phenomenon of twinning is described in Section 7.7.

inset of Figure 10.37. Under the influence of an applied stress, deformation of martensite (i.e., the passage from stage 2 to stage 3 in Figure 10.37) occurs by the migration of twin boundaries—some twinned regions grow while others shrink; this deformed martensitic structure is represented by the stage 3 inset. Furthermore, when the stress is removed, the deformed shape is retained at this temperature. Finally, upon subsequent heating to the initial temperature, the material reverts back to (i.e., “remembers”) its original size and shape (stage 4). This stage 3–stage 4 process is accompanied by a phase transformation from the deformed martensite into the original high-temperature austenite phase. For these shape-memory alloys, the martensite-to-austenite

transformation occurs over a temperature range, between the temperatures denoted by A_s (austenite start) and A_f (austenite finish) labels on the right vertical axis of Figure 10.37. This deformation–transformation cycle may be repeated for the shape-memory material.

The original shape (the one that is to be remembered) is created by heating to well above the A_f temperature (such that the transformation to austenite is complete) and then restraining the material to the desired memory shape for a sufficient time period. For example, for Nitinol alloys, a 1-h treatment at 500°C is necessary.

Although the deformation experienced by shape-memory alloys is semipermanent, it is not truly “plas-

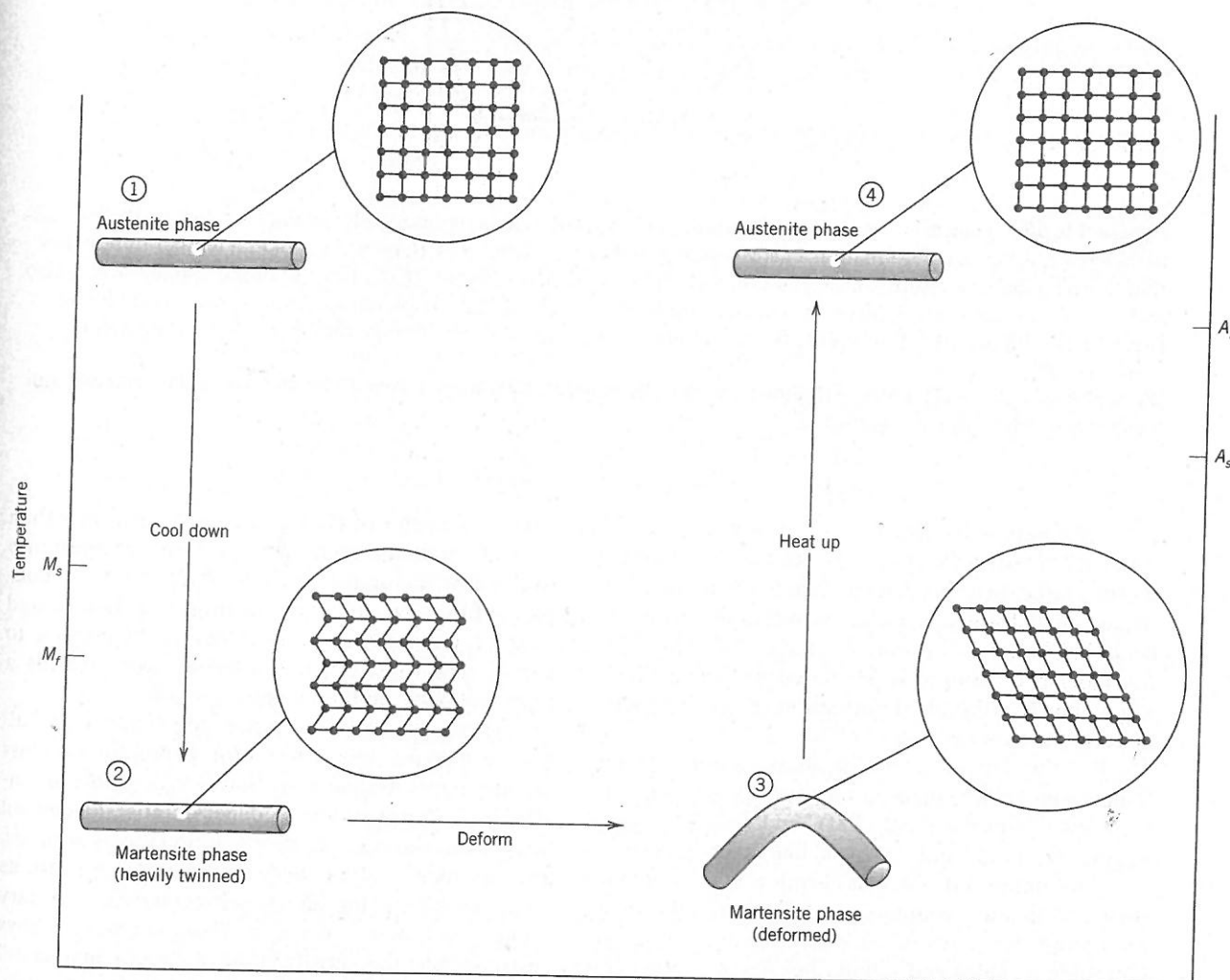


Figure 10.37 Diagram illustrating the shape-memory effect. The insets are schematic representations of the crystal structure at the four stages. M_s and M_f denote temperatures at which the martensitic transformation begins and ends, respectively. Likewise for the austenite transformation, A_s and A_f represent the respective beginning and end transformation temperatures.

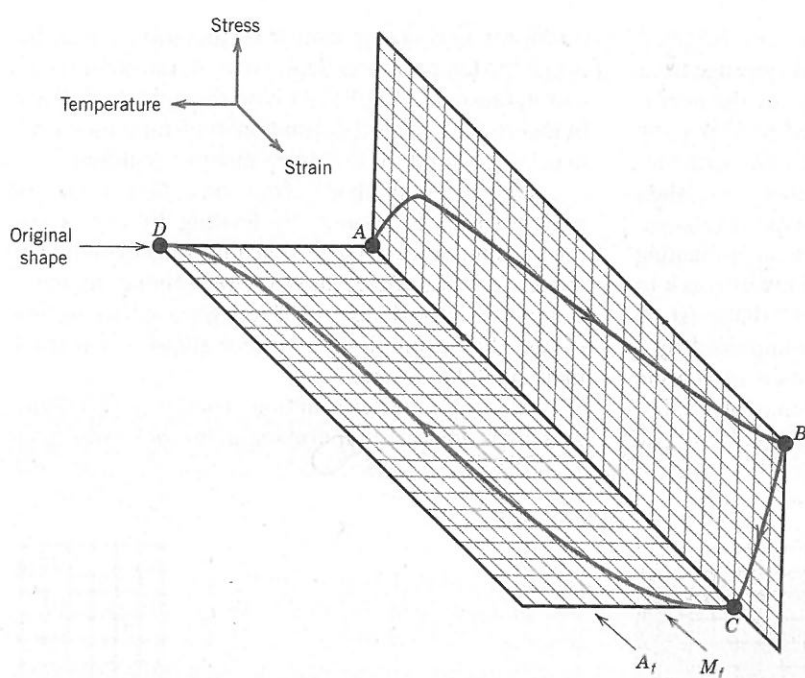


Figure 10.38 Typical stress-strain-temperature behavior of a shape-memory alloy, demonstrating its thermoelastic behavior. Specimen deformation, corresponding to the curve from A to B , is carried out at a temperature below that at which the martensitic transformation is complete (i.e., M_f of Figure 10.37). Release of the applied stress (also at M_f) is represented by the curve BC . Subsequent heating to above the completed austenite-transformation temperature (A_f , Figure 10.37) causes the deformed piece to resume its original shape (along the curve from point C to point D).

[From Helsen, J. A., and H. J. Breme (Editors), *Metals as Biomaterials*, John Wiley & Sons, Chichester, UK, 1998. Reprinted with permission of John Wiley & Sons Inc.]

tic” deformation, as discussed in Section 6.6, nor is it strictly “elastic” (Section 6.3). Rather, it is termed *thermoelastic*, because deformation is nonpermanent when the deformed material is subsequently heat-treated. The stress-strain-temperature behavior of a thermoelastic material is presented in Figure 10.38. Maximum recoverable deformation strains for these materials are on the order of 8%.

For this Nitinol family of alloys, transformation temperatures can be made to vary over a wide temperature range (between about -200°C and 110°C) by altering the Ni-Ti ratio and also by adding other elements.

One important SMA application is in weldless, shrink-to-fit pipe couplers used for hydraulic lines on aircraft, for joints on undersea pipelines, and for plumbing on ships and submarines. Each coupler (in the form of a cylindrical sleeve) is fabricated so as to have an inside diameter slightly smaller than the

outside diameter of the pipes to be joined. It is then stretched (circumferentially) at some temperature well below the ambient temperature. Next the coupler is fitted over the pipe junction and then heated to room temperature; heating causes the coupler to shrink back to its original diameter, thus creating a tight seal between the two pipe sections.

There is a host of other applications for alloys displaying this effect—for example, eyeglass frames, tooth-straightening braces, collapsible antennas, greenhouse window openers, antiscald control valves on showers, women’s foundation-garments, fire sprinkler valves, and biomedical applications (such as blood-clot filters, self-extending coronary stents, and bone anchors). Shape-memory alloys also fall into the classification of “smart materials” (Section 1.5) because they sense and respond to environmental (i.e., temperature) changes.

SUMMARY

The Kinetics of Phase Transformations

- Nucleation and growth are the two steps involved in the production of a new phase.
- Two types of nucleation are possible: homogeneous and heterogeneous.
 - For homogeneous nucleation, nuclei of the new phase form uniformly throughout the parent phase.
 - For heterogeneous nucleation, nuclei form preferentially at the surfaces of structural inhomogeneities (e.g., container surfaces, insoluble impurities).
- For the homogeneous nucleation of a spherical solid particle in a liquid solution, expressions for the critical radius (r^*) and activation free energy (ΔG^*) are represented by Equations 10.3 and 10.4, respectively. These two parameters are indicated in the plot of Figure 10.2b.
- The activation free energy for heterogeneous nucleation (ΔG_{het}^*) is lower than that for homogeneous nucleation (ΔG_{hom}^*), as demonstrated on the schematic free energy-versus-nucleus radius curves of Figure 10.6.
- Heterogeneous nucleation occurs more easily than homogeneous nucleation, which is reflected in a smaller degree of supercooling (ΔT) for the former—that is, $\Delta T_{\text{het}} < \Delta T_{\text{hom}}$, Figure 10.7.
- The growth stage of phase particle formation begins once a nucleus has exceeded the critical radius (r^*).
- For typical solid transformations, a plot of fraction transformation versus logarithm of time yields an S-shaped curve, as depicted schematically in Figure 10.10.
- The time dependence of degree of transformation is represented by the Avrami equation, Equation 10.17.
- Transformation rate is taken as the reciprocal of time required for a transformation to proceed halfway to its completion, Equation 10.18.
- For transformations that are induced by temperature alterations, when the rate of temperature change is such that equilibrium conditions are not maintained, transformation temperature is raised (for heating) and lowered (for cooling). These phenomena are termed superheating and supercooling, respectively.

Isothermal Transformation Diagrams

Continuous-Cooling Transformation Diagrams

- Phase diagrams provide no information as to the time dependence of transformation progress. However, the element of time is incorporated into isothermal transformation diagrams. These diagrams do the following:
 - Plot temperature versus the logarithm of time, with curves for beginning, as well as 50% and 100% transformation completion.
 - Are generated from a series of plots of percentage transformation versus the logarithm of time taken over a range of temperatures (Figure 10.13).
 - Are valid only for constant-temperature heat treatments.
 - Permit determination of times at which a phase transformation begins and ends.
- Isothermal transformation diagrams may be modified for continuous-cooling heat treatments; isothermal transformation beginning and ending curves are shifted to longer times and lower temperatures (Figure 10.25). Intersections with these curves of continuous-cooling curves represent times at which the transformation starts and ceases.

- Isothermal and continuous-cooling transformation diagrams make possible the prediction of microstructural products for specified heat treatments. This feature was demonstrated for alloys of iron and carbon.
- Microstructural products for iron–carbon alloys are as follows:
 - Coarse and fine pearlite—the alternating α -ferrite and cementite layers are thinner for fine than for coarse pearlite. Coarse pearlite forms at higher temperatures (isothermally) and for slower cooling rates (continuous cooling).
 - Bainite—this has a very fine structure that is composed of a ferrite matrix and elongated cementite particles. It forms at lower temperatures/higher cooling rates than fine pearlite.
 - Spheroidite—this is composed of spherelike cementite particles that are embedded in a ferrite matrix. Heating fine/coarse pearlite or bainite at about 700°C for several hours produces spheroidite.
 - Martensite—this has platelike or needle-like grains of an iron–carbon solid solution that has a body-centered tetragonal crystal structure. Martensite is produced by rapidly quenching austenite to a sufficiently low temperature so as to prevent carbon diffusion and the formation of pearlite and/or bainite.
 - Tempered martensite—this consists of very small cementite particles within a ferrite matrix. Heating martensite at temperatures within the range of about 250°C to 650°C results in its transformation to tempered martensite.
- The addition of some alloying elements (other than carbon) shifts pearlite and bainite noses on a continuous-cooling transformation diagram to longer times, making the transformation to martensite more favorable (and an alloy more heat-treatable).

Mechanical Behavior of Iron–Carbon Alloys

- Martensitic steels are the hardest and strongest, yet most brittle.
- Tempered martensite is very strong but relatively ductile.
- Bainite has desirable strength-ductility combination but is not as strong as tempered martensite.
- Fine pearlite is harder, stronger, and more brittle than coarse pearlite.
- Spheroidite is the softest and most ductile of the microstructures discussed.
- Embrittlement of some steel alloys results when specific alloying and impurity elements are present and upon tempering within a definite temperature range.

Shape-Memory Alloys

- These alloys may be deformed and then return to their predeformed sizes/shapes upon heating.
- Deformation occurs by the migration of twin boundaries. A martensite-to-austenite phase transformation accompanies the reversion back to the original size/shape.

Equation Summary

Equation Number	Equation	Solving For	Page Number
10.3	$r^* = -\frac{2\gamma}{\Delta G_v}$	Critical radius for stable solid particle (homogeneous nucleation)	360
10.4	$\Delta G^* = \frac{16\pi\gamma^3}{3(\Delta G_v)^2}$	Activation free energy for formation of stable solid particle (homogeneous nucleation)	360

(continued)

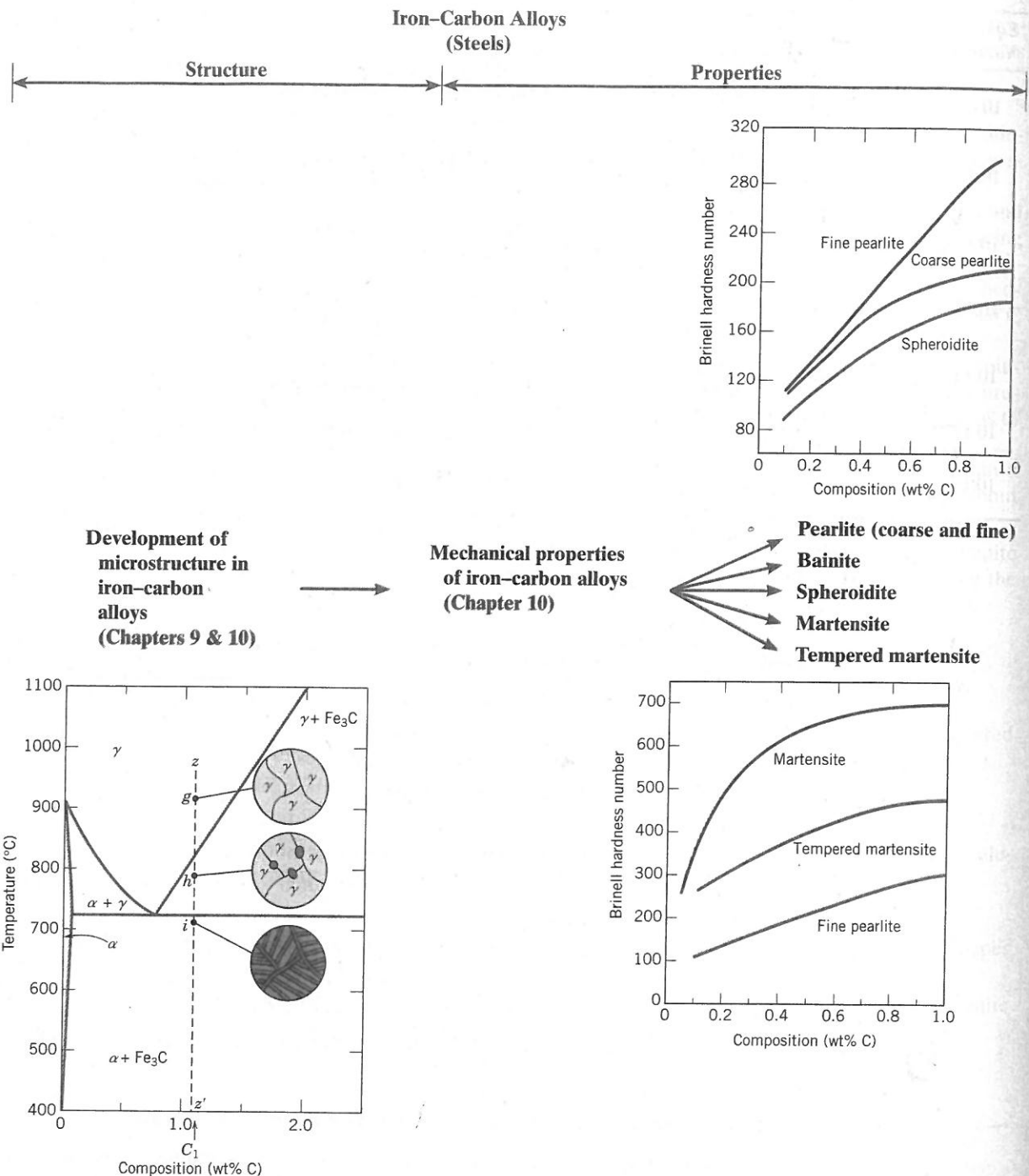
Equation Number	Equation	Solving For	Page Number
10.6	$r^* = \left(-\frac{2\gamma T_m}{\Delta H_f} \right) \left(\frac{1}{T_m - T} \right)$	Critical radius—in terms of latent heat of fusion and melting temperature	360
10.7	$\Delta G^* = \left(\frac{16\pi\gamma^3 T_m^2}{3\Delta H_f^2} \right) \frac{1}{(T_m - T)^2}$	Activation free energy—in terms of latent heat of fusion and melting temperature	360
10.12	$\gamma_{IL} = \gamma_{SI} + \gamma_{SL} \cos \theta$	Relationship among interfacial energies for heterogeneous nucleation	364
10.13	$r^* = -\frac{2\gamma_{SL}}{\Delta G_v}$	Critical radius for stable solid particle (heterogeneous nucleation)	364
10.14	$\Delta G^* = \left(\frac{16\pi\gamma_{SL}^3}{3\Delta G_v^2} \right) S(\theta)$	Activation free energy for formation of stable solid particle (heterogeneous nucleation)	364
10.17	$y = 1 - \exp(-kt^n)$	Fraction of transformation (Avrami equation)	368
10.18	$\text{rate} = \frac{1}{t_{0.5}}$	Transformation rate	368

List of Symbols

Symbol	Meaning
ΔG_v	Volume free energy
ΔH_f	Latent heat of fusion
k, n	Time-independent constants
$S(\theta)$	Nucleus shape function
T	Temperature (K)
T_m	Equilibrium solidification temperature (K)
$t_{0.5}$	Time required for a transformation to proceed to 50% completion
γ	Surface free energy
γ_{IL}	Liquid-surface interfacial energy (Figure 10.5)
γ_{SL}	Solid-liquid interfacial energy
γ_{SI}	Solid-surface interfacial energy
θ	Wetting angle (angle between γ_{SI} and γ_{SL} vectors) (Figure 10.5)

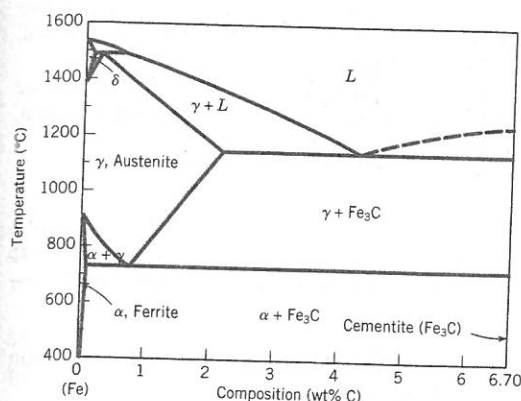
Processing/Structure/Properties/Performance Summary

For iron–carbon alloys, in addition to discussions of the heat treatments that produce the several microconstituents (fine/coarse pearlite, bainite, martensite, etc.) and their mechanical properties, correlations were made between mechanical properties and structural elements of these microconstituents. These correlations are indicated in the following concept map:

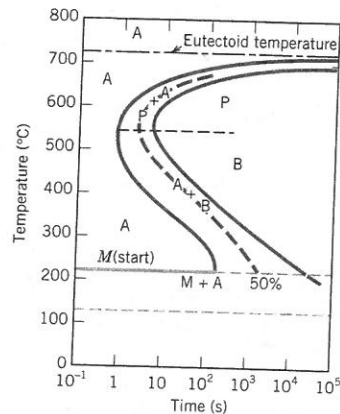


Furthermore, reference to the heat treating of steels (as discussed in Chapter 11) normally means tempering of martensite to form tempered martensite. An understanding of the conditions under which martensite forms is facilitated by utilizing continuous-cooling and isothermal transformation diagrams (Sections 10.5 and 10.6). In addition, these diagrams are just extensions of the iron–iron carbide phase diagram (Section 9.18). The following concept map notes these relationships:

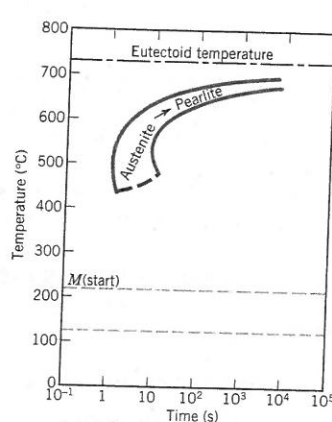
**Iron-Carbon Alloys
(Steels)
(Processing)**



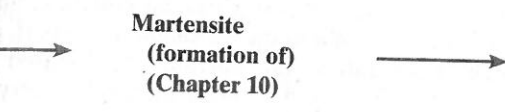
**Iron-iron carbide
phase diagram
(Chapter 9)**



**Isothermal
transformation
diagrams
(Chapter 10)**



**Continuous-cooling
transformation
diagrams
(Chapter 10)**

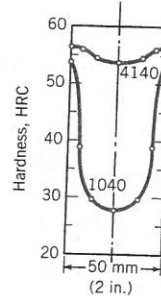


**Martensite
(formation of)
(Chapter 10)**

martensite (BCT, single phase) →
tempered martensite ($\alpha + \text{Fe}_3\text{C}$ phases)

**Tempering
(tempered
martensite)
(Chapter 10)**

**Heat treatment
of steels
(Chapter 11)**



Important Terms and Concepts

alloy steel
athermal transformation
bainite
coarse pearlite
continuous-cooling
transformation diagram
fine pearlite
free energy

growth (phase particle)
isothermal transformation
diagram
kinetics
martensite
nucleation
phase transformation
plain carbon steel

spheroidite
supercooling
superheating
tempered martensite
thermally activated
transformation
transformation rate

REFERENCES

- Brooks, C. R., *Principles of the Heat Treatment of Plain Carbon and Low Alloy Steels*, ASM International, Materials Park, OH, 1996.
- Krauss, G., *Steels: Processing, Structure, and Performance*, ASM International, Materials Park, OH, 2005.
- Porter, D. A., K. E. Easterling, and M. Sherif, *Phase Transformations in Metals and Alloys*, 3rd edition, CRC Press, Boca Raton, FL, 2009.
- Shewmon, P. G., *Transformations in Metals*, Indo American Books, Abbotsford, B.C., Canada, 2007.
- Tarin, P., and J. Pérez, *SteCal® 3.0* (Book and CD), ASM International, Materials Park, OH, 2004.
- Vander Voort, G. (Editor), *Atlas of Time-Temperature Diagrams for Irons and Steels*, ASM International, Materials Park, OH, 1991.
- Vander Voort, G. (Editor), *Atlas of Time-Temperature Diagrams for Nonferrous Alloys*, ASM International, Materials Park, OH, 1991.

QUESTIONS AND PROBLEMS

⊕ Problem available (at instructor's discretion) in WileyPLUS

The Kinetics of Phase Transformations

10.1 Name the two stages involved in the formation ⊕ of particles of a new phase. Briefly describe each.

10.2 (a) Rewrite the expression for the total free energy change for nucleation (Equation 10.1) for the case of a cubic nucleus of edge length a (instead of a sphere of radius r). Now differentiate this expression with respect to a (per Equation 10.2) and solve for both the critical cube edge length, a^* , and ΔG^* .

(b) Is ΔG^* greater for a cube or a sphere? Why?

10.3 If ice homogeneously nucleates at -40°C , calculate the critical radius given values of $-3.1 \times 10^8 \text{ J/m}^3$ and $25 \times 10^{-3} \text{ J/m}^2$, respectively, for the latent heat of fusion and the surface free energy.

10.4 (a) For the solidification of nickel, calculate the ⊕ critical radius r^* and the activation free energy ΔG^* if nucleation is homogeneous. Values for the latent heat of fusion and surface free energy are $-2.53 \times 10^9 \text{ J/m}^3$ and 0.255 J/m^2 , respectively. Use the supercooling value found in Table 10.1.

(b) Now, calculate the number of atoms found in a nucleus of critical size. Assume a lattice parameter of 0.360 nm for solid nickel at its melting temperature.

10.5 (a) Assume for the solidification of nickel (Problem 10.4) that nucleation is homogeneous and that the number of stable nuclei is 10^6 nuclei per cubic meter. Calculate the critical radius and the number of stable nuclei that exist at the following degrees of supercooling: 200 and 300 K.

(b) What is significant about the magnitudes of these critical radii and the numbers of stable nuclei?

10.6 For some transformation having kinetics that ⊕ obey the Avrami equation (Equation 10.17), the parameter n is known to have a value of 1.5. If the reaction is 25% complete after 125 s, how

long (total time) will it take the transformation to go to 90% completion?

10.7 Compute the rate of some reaction that obeys

⊕ Avrami kinetics, assuming that the constants n and k have values of 2.0 and 5×10^{-4} , respectively, for time expressed in seconds.

10.8 It is known that the kinetics of recrystallization

⊕ for some alloy obeys the Avrami equation, and that the value of n in the exponential is 5.0. If, at some temperature, the fraction recrystallized is 0.30 after 100 min, determine the rate of recrystallization at this temperature.

10.9 It is known that the kinetics of some transformation obeys the Avrami equation and that the value of k is 2.6×10^{-6} (for time in minutes). If the fraction recrystallized is 0.65 after 120 min, determine the rate of this transformation.

10.10 The kinetics of the austenite-to-pearlite trans-

⊕ formation obeys the Avrami relationship. Using the fraction transformed-time data given here, determine the total time required for 95% of the austenite to transform to pearlite.

Fraction Transformed	Time (s)
0.2	280
0.6	425

10.11 The fraction recrystallized-time data for the

⊕ recrystallization at 350°C of a previously deformed aluminum are tabulated here. Assuming that the kinetics of this process obey the Avrami relationship, determine the fraction recrystallized after a total time of 116.8 min.

Fraction Recrystallized	Time (min)
0.30	95.2
0.80	126.6

- 10.12** (a) From the curves shown in Figure 10.11 and using Equation 10.18, determine the rate of recrystallization for pure copper at the several temperatures.
 (b) Make a plot of $\ln(\text{rate})$ versus the reciprocal of temperature ($\text{in } \text{K}^{-1}$), and determine the activation energy for this recrystallization process. (See Section 5.5.)
 (c) By extrapolation, estimate the length of time required for 50% recrystallization at room temperature, 20°C (293 K).

- 10.13** Determine values for the constants n and k (Equation 10.17) for the recrystallization of copper (Figure 10.11) at 119°C .

Metastable versus Equilibrium States

- 10.14** In terms of heat treatment and the development of microstructure, what are two major limitations of the iron–iron carbide phase diagram?

- 10.15** (a) Briefly describe the phenomena of superheating and supercooling.
 (b) Why do these phenomena occur?

Isothermal Transformation Diagrams

- 10.16** Suppose that a steel of eutectoid composition is cooled to 675°C (1250°F) from 760°C (1400°F) in less than 0.5 s and held at this temperature.

- (a) How long will it take for the austenite-to-pearlite reaction to go to 50% completion? To 100% completion?
 (b) Estimate the hardness of the alloy that has completely transformed to pearlite.

- 10.17** Briefly cite the differences among pearlite, bainite, and spheroidite relative to microstructure and mechanical properties.

- 10.18** What is the driving force for the formation of spheroidite?

- 10.19** Using the isothermal transformation diagram for an iron–carbon alloy of eutectoid composition (Figure 10.22), specify the nature of the final microstructure (in terms of microconstituents present and approximate percentages of each) of a small specimen that has been subjected to the following time–temperature treatments. In each case assume that the specimen begins at 760°C (1400°F) and that it has been held at this temperature long enough to have achieved a complete and homogeneous austenitic structure.

- (a) Cool rapidly to 350°C (660°F), hold for 10^3 s, then quench to room temperature.
 (b) Rapidly cool to 625°C (1160°F), hold for 10 s, then quench to room temperature.

- (c) Rapidly cool to 600°C (1110°F), hold for 4 s, rapidly cool to 450°C (840°F), hold for 10 s, then quench to room temperature.

- (d) Reheat the specimen in part (c) to 700°C (1290°F) for 20 h.

- (e) Rapidly cool to 300°C (570°F), hold for 20 s, then quench to room temperature in water. Reheat to 425°C (800°F) for 10^3 s and slowly cool to room temperature.

- (f) Cool rapidly to 665°C (1230°F), hold for 10^3 s, then quench to room temperature.

- (g) Rapidly cool to 575°C (1065°F), hold for 20 s, rapidly cool to 350°C (660°F), hold for 100 s, then quench to room temperature.

- (h) Rapidly cool to 350°C (660°F), hold for 150 s, then quench to room temperature.

- 10.20** Make a copy of the isothermal transformation diagram for an iron–carbon alloy of eutectoid composition (Figure 10.22) and then sketch and label time–temperature paths on this diagram to produce the following microstructures:

(a) 100% coarse pearlite

(b) 50% martensite and 50% austenite

(c) 50% coarse pearlite, 25% bainite, and 25% martensite

- 10.21** Using the isothermal transformation diagram for a 1.13 wt% C steel alloy (Figure 10.39), determine the final microstructure (in terms of just the microconstituents present) of a small specimen that has been subjected to the following time–temperature treatments. In each case assume that the specimen begins at 920°C (1690°F) and that it has been held at this temperature long enough to have achieved a complete and homogeneous austenitic structure.

- (a) Rapidly cool to 250°C (480°F), hold for 10^3 s, then quench to room temperature.

- (b) Rapidly cool to 775°C (1430°F), hold for 500 s, then quench to room temperature.

- (c) Rapidly cool to 400°C (750°F), hold for 500 s, then quench to room temperature.

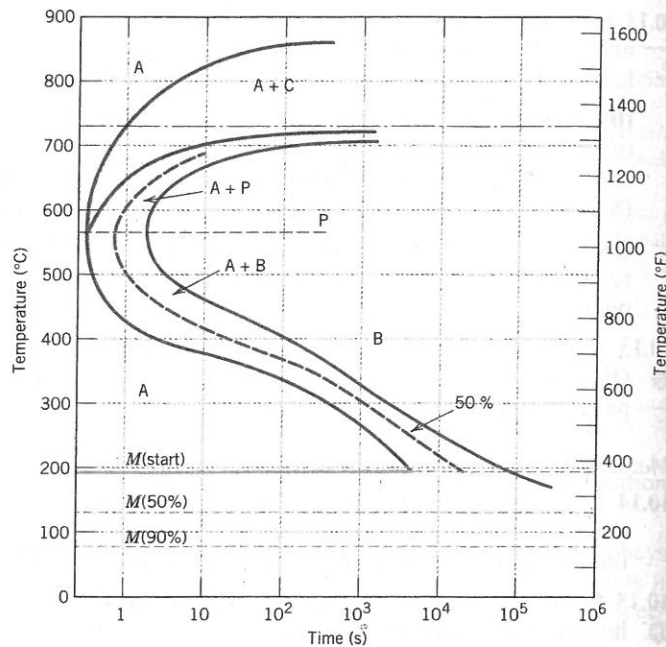
- (d) Rapidly cool to 700°C (1290°F), hold at this temperature for 10^5 s, then quench to room temperature.

- (e) Rapidly cool to 650°C (1200°F), hold at this temperature for 3 s, rapidly cool to 400°C (750°F), hold for 25 s, then quench to room temperature.

- (f) Rapidly cool to 350°C (660°F), hold for 300 s, then quench to room temperature.

Figure 10.39 Isothermal transformation diagram for a 1.13 wt% C iron–carbon alloy: A, austenite; B, bainite; C, proeutectoid cementite; M, martensite; P, pearlite.

[Adapted from H. Boyer (Editor), *Atlas of Isothermal Transformation and Cooling Transformation Diagrams*, 1977. Reproduced by permission of ASM International, Materials Park, OH.]



(g) Rapidly cool to 675°C (1250°F), hold for 7 s, then quench to room temperature.

(h) Rapidly cool to 600°C (1110°F), hold at this temperature for 7 s, rapidly cool to 450°C (840°F), hold at this temperature for 4 s, then quench to room temperature.

10.22 For parts a, c, d, f, and h of Problem 10.21, determine the approximate percentages of the microconstituents that form.

10.23 Make a copy of the isothermal transformation diagram for a 1.13 wt% C iron–carbon alloy (Figure 10.39), and then on this diagram sketch and label time–temperature paths to produce the following microstructures:

- (a) 6.2% proeutectoid cementite and 93.8% coarse pearlite
- (b) 50% fine pearlite and 50% bainite
- (c) 100% martensite
- (d) 100% tempered martensite

Continuous-Cooling Transformation Diagrams

10.24 Name the microstructural products of eutectoid iron–carbon alloy (0.76 wt% C) specimens that are first completely transformed to austenite, then cooled to room temperature at the following rates:

- | | |
|------------|-------------|
| (a) 1°C/s | (c) 50°C/s |
| (b) 20°C/s | (d) 175°C/s |

10.25 Figure 10.40 shows the continuous-cooling transformation diagram for a 0.35 wt% C iron–carbon alloy. Make a copy of this figure, and then sketch and label continuous-cooling curves to yield the following microstructures:

- (a) Fine pearlite and proeutectoid ferrite
- (b) Martensite
- (c) Martensite and proeutectoid ferrite
- (d) Coarse pearlite and proeutectoid ferrite
- (e) Martensite, fine pearlite, and proeutectoid ferrite

10.26 Cite two important differences between continuous-cooling transformation diagrams for plain carbon and alloy steels.

10.27 Briefly explain why there is no bainite transformation region on the continuous-cooling transformation diagram for an iron–carbon alloy of eutectoid composition.

10.28 Name the microstructural products of 4340 alloy steel specimens that are first completely transformed to austenite, then cooled to room temperature at the following rates:

- (a) 0.005°C/s
- (b) 0.05°C/s
- (c) 0.5°C/s
- (d) 5°C/s

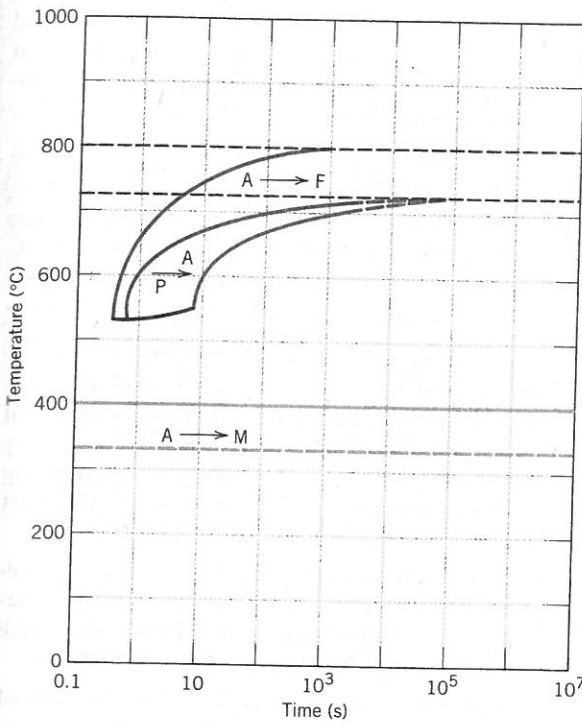


Figure 10.40 Continuous-cooling transformation diagram for a 0.35 wt% C iron–carbon alloy.

10.29 Briefly describe the simplest continuous-cooling heat treatment procedure that would be used in converting a 4340 steel from one microstructure to another.

- (a) (Martensite + ferrite + bainite) to (martensite + ferrite + pearlite + bainite)
- (b) (Martensite + ferrite + bainite) to spheroidite
- (c) (Martensite + bainite + ferrite) to tempered martensite

10.30 On the basis of diffusion considerations, explain why fine pearlite forms for the moderate cooling of austenite through the eutectoid temperature, whereas coarse pearlite is the product for relatively slow cooling rates.

Mechanical Behavior of Iron–Carbon Alloys Tempered Martensite

10.31 Briefly explain why fine pearlite is harder and stronger than coarse pearlite, which in turn is harder and stronger than spheroidite.

10.32 Cite two reasons why martensite is so hard and brittle.

10.33 Rank the following iron–carbon alloys and associated microstructures from the hardest to the softest:

- (a) 0.25 wt% C with coarse pearlite
- (b) 0.80 wt% C with spheroidite
- (c) 0.25 wt% C with spheroidite
- (d) 0.80 wt% C with fine pearlite.

Justify this ranking.

10.34 Briefly explain why the hardness of tempered martensite diminishes with tempering time (at constant temperature) and with increasing temperature (at constant tempering time).

10.35 Briefly describe the simplest heat treatment procedure that would be used in converting a 0.76 wt% C steel from one microstructure to the other, as follows:

- (a) Martensite to spheroidite
- (b) Spheroidite to martensite
- (c) Bainite to pearlite
- (d) Pearlite to bainite
- (e) Spheroidite to pearlite
- (f) Pearlite to spheroidite
- (g) Tempered martensite to martensite
- (h) Bainite to spheroidite

10.36 (a) Briefly describe the microstructural difference between spheroidite and tempered martensite.

- (b) Explain why tempered martensite is much harder and stronger.

10.37 Estimate Brinell hardnesses and ductilities (%RA) for specimens of an iron–carbon alloy of eutectoid composition that have been subjected to the heat treatments described in parts (a) through (h) of Problem 10.19.

10.38 Estimate the Brinell hardnesses for specimens of a 1.13 wt% C iron–carbon alloy that have been subjected to the heat treatments described in parts (a), (d), and (h) of Problem 10.21.

10.39 Determine the approximate tensile strengths and ductilities (%RA) for specimens of a eutectoid iron–carbon alloy that have experienced the heat treatments described in parts (a) through (d) of Problem 10.24.

Spreadsheet Problem

10.1SS For some phase transformation, given at least two values of fraction transformation and their corresponding times, generate a spreadsheet that will allow the user to determine the following:

- (a) the values of n and k in the Avrami equation
- (b) the time required for the transformation to proceed to some degree of fraction transformation

- (c) the fraction transformation after some specified time has elapsed

DESIGN PROBLEMS

Continuous-Cooling Transformation Diagrams

Mechanical Behavior of Iron-Carbon Alloys

- 10.D1** Is it possible to produce an iron-carbon alloy of eutectoid composition that has a minimum hardness of 200 HB and a minimum ductility of 25%RA? If so, describe the continuous-cooling heat treatment to which the alloy would be subjected to achieve these properties. If it is not possible, explain why.
- 10.D2** For a eutectoid steel, describe isothermal heat treatments that would be required to yield specimens having the following tensile strength-ductility (%RA) combinations:
- 900 MPa and 30%RA
 - 700 MPa and 25%RA
- 10.D3** For a eutectoid steel, describe isothermal heat treatments that would be required to yield specimens having the following tensile strength-ductility (%RA) combinations:
- 1800 MPa and 30%RA
 - 1700 MPa and 45%RA
 - 1400 MPa and 50%RA
- 10.D4** For a eutectoid steel, describe continuous-cooling heat treatments that would be required to yield specimens having the following Brinell hardness-ductility (%RA) combinations:
- 680 HB and ~0%RA
 - 260 HB and 20%RA
 - 200 HB and 28%RA
 - 160 HB and 67%RA
- 10.D5** Is it possible to produce an iron-carbon alloy that has a minimum tensile strength of 620 MPa (90,000 psi) and a minimum ductility of 50% RA? If so, what will be its composition and microstructure (coarse and fine pearlites and spheroidite are alternatives)? If this is not possible, explain why.
- 10.D6** It is desired to produce an iron-carbon alloy that has a minimum hardness of 200 HB and a minimum ductility of 35% RA. Is such an alloy
- possible? If so, what will be its composition and microstructure (coarse and fine pearlites and spheroidite are alternatives)? If this is not possible, explain why.

Tempered Martensite

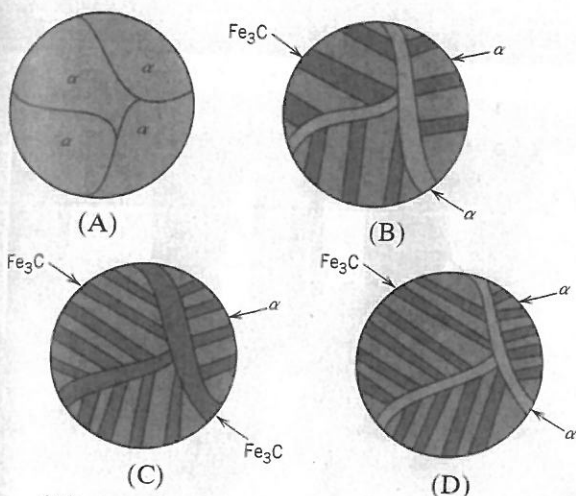
- 10.D7 (a)** For a 1080 steel that has been water quenched, estimate the tempering time at 535°C (1000°F) to achieve a hardness of 45 HRC.
- (b)** What will be the tempering time at 425°C (800°F) necessary to attain the same hardness?
- 10.D8** An alloy steel (4340) is to be used in an application requiring a minimum tensile strength of 1515 MPa (220,000 psi) and a minimum ductility of 40%RA. Oil quenching followed by tempering is to be used. Briefly describe the tempering heat treatment.
- 10.D9** For a 4340 steel alloy, describe continuous-cooling/tempering heat treatments that would be required to yield specimens having the following yield/tensile strength-ductility property combinations:
- tensile strength of 1100 MPa, ductility of 50%RA
 - yield strength of 1200 MPa, ductility of 45%RA
 - tensile strength of 1300 MPa, ductility of 45%RA
- 10.D10** Is it possible to produce an oil-quenched and tempered 4340 steel that has a minimum yield strength of 1240 MPa (180,000 psi) and a ductility of at least 50%RA? If this is possible, describe the tempering heat treatment. If it is not possible, then explain why.

FUNDAMENTALS OF ENGINEERING QUESTIONS AND PROBLEMS

- 10.1FE** Which of the following describes recrystallization?
- Diffusion dependent with a change in phase composition
 - Diffusionless
 - Diffusion dependent with no change in phase composition
 - All of the above

- 10.2FE** Schematic room-temperature microstructures for four iron-carbon alloys are as follows.

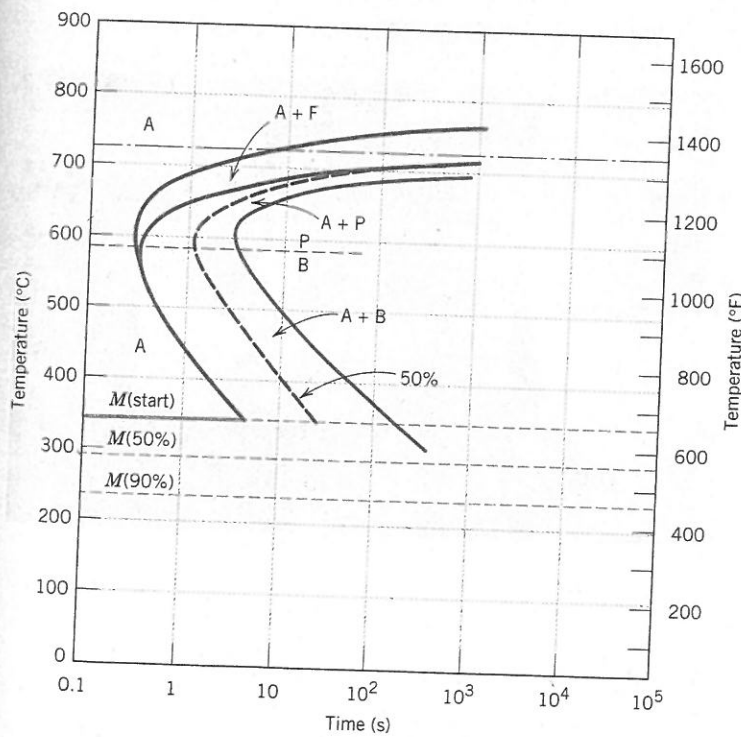
Rank these microstructures (by letter) from the hardest to the softest.



- (A) A > B > C > D
- (B) C > D > B > A
- (C) A > B > D > C
- (D) None of the above

10.3FE On the basis of the accompanying isothermal transformation diagram for a 0.45 wt% C iron-carbon alloy, which heat treatment could be used to isothermally convert a microstructure that consists of proeutectoid ferrite and fine pearlite into one that is composed of proeutectoid ferrite and martensite?

- (A) Austenitize the specimen at approximately 700°C, rapidly cool to about 675°C, hold at this temperature for 1 to 2 s, and then rapidly quench to room temperature
- (B) Rapidly heat the specimen to about 675°C, hold at this temperature for 1 to 2 s, then rapidly quench to room temperature
- (C) Austenitize the specimen at approximately 775°C, rapidly cool to about 500°C, hold at this temperature for 1 to 2 s, and then rapidly quench to room temperature
- (D) Austenitize the specimen at approximately 775°C, rapidly cool to about 675°C, hold at this temperature for 1 to 2 s, and then rapidly quench to room temperature



Isothermal transformation diagram for a 0.45 wt% C iron-carbon alloy:
 A, austenite; B, bainite; F, proeutectoid ferrite; M, martensite; P, pearlite.
 (Adapted from *Atlas of Time-Temperature Diagrams for Irons and Steels*, G. F. Vander Voort, Editor, 1991. Reprinted by permission of ASM International, Materials Park, OH.)